DOI 10.1007/s10527-016-9550-1
Biomedical Engineering, Vol. 49, No. 5, January, 2016, pp. 288-291. Translated from Meditsinskaya Tekhnika, Vol. 49, No. 5, Sep.-Oct., 2015, pp. 25-28.
Original article submitted August 5, 2015.

Development of New Sensitive Broadband Elements of Sensors Based on Carbon Nanotubes

E. V. Blagov[1]*, A. Yu. Gerasimenko[2], A. A. Dudin[1], L. P. Ichkitidze[2], E. P. Kitsuk[3], A. P. Orlov[1,4], A. A. Pavlov[1], A. A. Polokhin[2], and Yu. P. Shaman[3]

A new type of sensitive elements based on carbon nanotubes (SECNT) was developed for photoelectric detectors of optical radiation. The optical parameters of the SECNT were tested. The working wavelength range was found to be 500-8000 nm. The maximum photosensitivity of the SECNT reached 0.7 mA/W in the near-IR range of the spectrum. The time resolution of the sensitive element was no worse than 30 μsec.

Introduction

Contemporary biomedical engineering makes extensive use of optical systems. Diagnostic optical systems are used in ophthalmology, tomography, topography of the human body, laboratory microbiology research, etc. Therapeutic optical systems provide evaporation, coagulation, and cutting of biological tissues, intravenous exposure of blood, control of addressed transport of drugs, etc. The use of optical systems in biomedical engineering provides a basis for control of optical radiation.

Since the early 1900s, detectors of optical radiation based on different physical principles have been developed. The majority of available detectors are based on only three physical principles: thermal photodetectors, detectors based on external photoeffect, and detectors based on internal photoeffect.

A sensitive element intended to absorb radiation is the main element of the photodetector. According to the principle of action, the sensitive elements fall into two basic types: photothermal and photoelectric. Photodetectors of the first and second types convert light energy into thermal and electric energy, respectively. Photothermal detectors have high inertia and depend on environmental conditions [1].

The second type of photodetector provides direct conversion of incident light energy into electrical energy. Such photodetectors can implement external photoeffect. They are designed as electrovacuum (emission) devices with sensitive photocathode elements. These photoemission elements provide low efficiency of conversion (10%). Similar photodetectors can use the internal photoeffect: photosensitivity of the sensitive element depends on concentration of non-equilibrium charge that is generated by light. The internal photoeffect is typical of semiconductors. The main disadvantage of semiconductor photodetectors is the small range of working wavelengths. The top wavelength of photodetectors based on GaInAsSb/GaAlAsSb is 2550 nm. But these photodetectors are not presently commercially available [2].

Carbon nanotubes (CNT) of semiconductor type can be used as semiconductor material for sensitive elements. Unique structure and properties of CNT provide their promising use in nanoelectronics and nanodevices (including sensitive elements of broad-range IR photodetectors) [3, 4].

The CNT-based photodetectors fall into three types: based on a single carbon nanotube [5, 6], CNT films [5, 7], and CNT mass [8, 9]. It is difficult to construct sensitive elements based on a single carbon nanotube because of low electromotive force between two electrodes. Practical implementation of the sensitive element based on CNT

[1] Institute of Microelectronic Nanotechnology, Russian Academy of Sciences, Moscow, Russia; E-mail: nanobiomedics@gmail.com
[2] National Research University of Electronic Technology, Zelenograd, Moscow, Russia.
[3] SPC "Technological Center" MIET, Zelenograd, Moscow, Russia.
[4] Kotelnikov Institute of Radio-engineering and Electronics, Russian Academy of Sciences, Moscow, Russia.
* To whom correspondence should be addressed.

films is easier to achieve. However, CNT films are difficult to be structured with respect to volume, thereby making it difficult to measure low-intensity radiation. Synthesis of structured CNT-based mass between electrodes avoids the disadvantages of the two types of photodetectors.

Materials and Methods

A technology for development and testing of optical parameters of sensitive elements of emission photodetectors based on mass multilayer CNT nanotubes is discussed in this work.

The two-electrode system (cell matrix with mass CNT structures) was selected as the main working topology of sensitive element based on CNT (SECNT) structures. The holes of the cells were 2 μm in diameter and 2.3 μm in depth. The top electrode is a 0.5-μm metal layer coated with pure aluminum using the magnetron diffusion method. Lithography metallization forms a contact zone. A silicon plate is used as the bottom electrode (substrate) for the whole structure. The substrate is made of KEF 4.5 Ω/cm and KEM 0.001-0.002 Ω/cm silicon with electronic conductivity. A silicon oxide (SiO_2) layer (0.5 μm) is used as the dielectric. The dielectric is formed using thermal oxidation of silicon. The SECNT is a square matrix 2 mm in size (6 μm between cells).

The cell matrix is formed by selective plasmochemical etching of Al and silicon oxide in the Platran 100 experimental apparatus with high-density plasma of high reactivity. The cells are further etched with silicon in the BOSCH-etching apparatus. The SiO_2 layer is etched to the depth 0.2 μm using the gas phase etching method. The contact between silicon and CNT is maintained at the necessary level with deepening of CNT mass inside the structure. At the final stage of the procedure, the silicon plate is divided into crystals for synthesis of CNT mass.

The Al/Ni catalytic pair was selected experimentally to provide the maximal yield of IR radiation. The selection of Al was determined by its burning into silicon and generation of heterogenic transition CNT–silicon. As Al is effectively dissolved in silicon and Ni is expended during CNT growth, direct contact between CNT and silicon is formed. Given the requirements of radiation propagation to the contact CNT–silicon, the synthesis parameters depth and mass density are specified. The metal catalyst layers are applied to metal targets using magnetron spraying of metals in the URM 3.279.026 reactive ion-plasma evaporation apparatus. The metal catalyst layers are removed from the plate surface using ion-etching methods.

CNT mass synthesis temperature was below 500°C to prevent Al metallization damage. The synthesis method is plasma-stimulated chemical vapor sedimentation, which reduces synthesis temperature below 500°C with constant morphology of CNT mass. CNT growth rate is 5 μm/min, which allows nanotubes of 0.3-30 μm to be formed with homogeneous substrate. Mass density control is mediated by electric field.

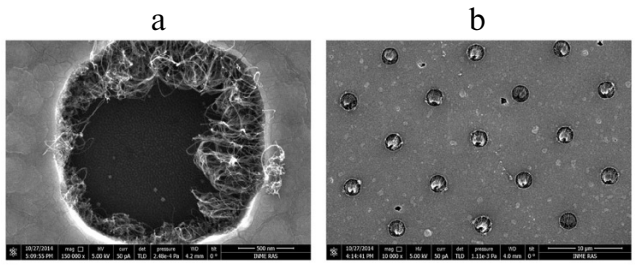

Fig. 1. Images of scanning electron micrograph of single cell (a) and segment with SECNT cells with synthesized CNT (b).

CNT mass is synthesized in the Oxford PlasmaLab System 100 (Nanofab 800 Agile). High purity grade of gases used in the synthesis provide high process stability and reduced defects of carbon multilayer nanotubes.

Analysis of synthesized structure of sensitive element using the FEI Helios NanoLab 650 scanning electron-ion microscope demonstrated that with similar synthesis parameters of CNT, mass growth in horizontal direction was larger than in vertical direction (vertical mass was synthesized strictly upward). This is probably due either to ineffective migration of carbon-containing agents into the cell or the effect of electric field on the synthesis in horizontal projection.

Preliminary research revealed that IR-induced effect is observed not only in case of vertical orientation of tubes, but also in case of horizontal orientation. In the latter case, CNT synthesis is mainly observed along the side surface of the elements. In this cases, lower density of CNT mass correspond to longer individual nanotubes (Fig. 1).

An automatic control system of SECNT production guarantees process reproducibility and the absence of variation of parameters due to operator activity.

Results

Basic optical parameters of photodetectors based on SECNT (working range of wavelengths, photosensitivity, and time resolution) were tested. A device based on optical and electrical control components was constructed. The device is controlled using LabVIEW software.

The working wavelength range is determined by detecting photoelectromotive force at the SECNT induced

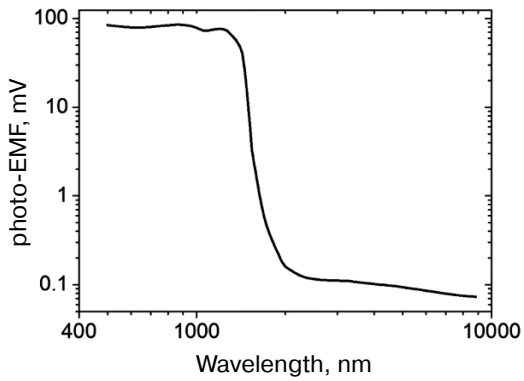

Fig. 2. Dependence of wavelength of photoelectromotive force on incident light applied to a SECNT.

by incident light. Working wavelength range of SECNT was measured using an MDR-41 spectrometric monochromator (OCB-Spektr, St. Petersburg). The optical system contains two halogenic light sources (λ = 370-2500 nm) and an absolute black body (λ = 2000-25000 nm). The input beam is formed using mirror condenser and glass filters. The output beam is formed by the output monochromator slit and a second condenser. The output beam power was calibrated using the Ophir 3A-FS standard thermal power meter. The photovoltage or photocurrent was measured using the combined system containing source and a Keithley SourceMeter 2634B instrument.

The experiments were focused on elucidation of the dependence of photoelectromotive force of the SECNT on the wavelength of incident light (Fig. 2). Figure 2 shows that the maximal photoelectromotive force of 110 mV was observed in visible and near-IR ranges 500-1500 nm. Perhaps, this is due to the size of the electrovoltaic cells (diameter and depth) and diameter of the CNT. Within the range 1500-8000 nm, the photoelectromotive force dropped to 0.1 mV.

The photosensitivity of the SECNT is the ratio of photocurrent divided by power of incident light on the SECNT. The photosensitivity of the SECNT was tested at three wavelengths (500, 800, 1100 nm), which are most frequently used in medicine. The power of light at given wavelengths was modified using neutral glass filters and controlled by the Ophir 3A-FS standard calibrated photodetector. The dependence of the photocurrent on the power of incident light at given wavelength was measured using the Keithley 2634B (Fig. 3). Figure 3 shows that the sensitivity of the SECNT at 500 nm (curve 1) is 7.1 mA/W at light power 50 μW. At the wavelengths of 800 (curve 2) and 1100 nm (curve 3), the SECNT sensitivity of the same sample was 7.4 and 12.2 mA/W, respectively.

The SECNT response time was monitored as follows. A pulse generator provided a power pulse of 3 V amplitude, which was applied to the LED. The IR-radiation (940 nm) generated by LED with fast fronts (<10 nsec) was applied to the SECNT. The oscillograms of the pulse generator and SECNT photoelectromotive force were compared to each other. The response time was calculated as the sum of delay time of the generator pulse and time of pulse front rise to 0.9 of maximal voltage amplitude.

The SECNT signal delay time relative to generator signal tends to a minimum value (<100 nsec). Thus, the SECNT response time can be characterized by the voltage rise time. It was determined from our experiments that the characteristic SECNT response time was 30 μsec. Perhaps this value is due to large contact resistance and capacitance as well as mismatch of oscilloscope input impedance (1 MΩ) with samples. Due to technological upgrade, these contact parameters can be optimized.

Conclusion

A new type of sensitive element for photoemission detectors of visible and IR-radiation is described. The sensitive elements were implemented as two-electrode matrix with integral masses of multicell CNT. The diameter of the SECNT cells was 2 μm; the depth was 2.3 μm. The top electrode of the system was 0.5 μm layer of pure Al; the bottom electrode was silicon plate with electron conductivity. A 0.5 μm layer of silicon oxide (SiO_2) was used as dielectric. The SECNT is a square matrix 2 mm in size. The distance between the matrix cells is 6 μm.

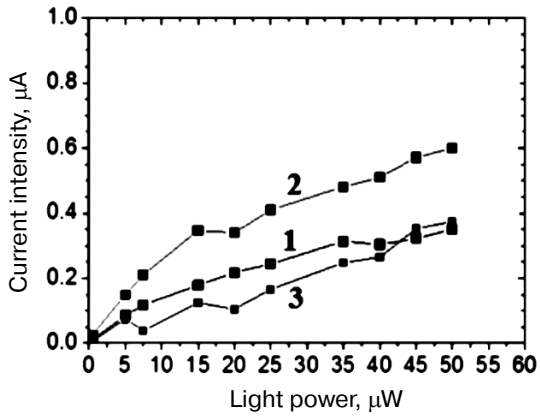

Fig. 3. Dependence of photocurrent of an SECNT on power of incident light at different wavelengths (nm): 1) 500; 2) 800; 3) 1100.

The optical parameters of the SECNT were tested. The working wavelength range for the maximal photoelectromotive force was observed in visible and near-IR ranges 500-1500 nm, which accounted for 110 mV. The photoelectromotive force within the range 1500-8000 nm dropped to 0.1 mV. Perhaps, such spectral distribution of photoelectromotive force was due to the size (diameter and depth) of matrix cells, as well as the diameter of single CNT in the sample composed of conductors connecting two electrodes.

The dependence of the sample current on light power (photosensitivity) was measured at wavelengths of 500, 800, and 1100 nm. The SECNT photosensitivity at 500 nm was up to 0.33 mA/W at light power 50 μW. In the same sample tested at 800 and 1100 nm, the photosensitivity was 0.7 and 0.175 mA/W, respectively. Thus, the maximal photosensitivity was observed at 800 nm.

The research into SECNT response time demonstrated that the signal delay time relative to generator signal tended to a minimum value (<100 nsec). The response time was mainly characterized by voltage rise time. It was demonstrated in our experiments that the time resolution of the SECNT is 30 μsec. Perhaps, this value is due to large contact resistance and capacitance as well as mismatch of oscilloscope input impedance (1 MΩ) with samples.

Further research will be focused on optimization of technological parameters intended to increase the working range of the wavelength as well as photosensitivity and speed of response of the SECNT. The optimization includes SECNT surface purification from undesirable carbon sediments and removal of defect layers of multicell carbon nanotubes, which increases the system quality and provides light permeation to the CNT–silicon contact. Although the optimization should further improve the performance of the photoemission detector of visible and IR-radiation based on SECNT, the detector can already be successfully used for optical radiation detection in diagnostic or therapeutic medical systems.

This work was supported by the Russian Ministry of Education and Science (Project No. 14.430.11.0006).

REFERENCES

1. Vesnin V.L., Muradov V.G., Izv. SNTs RAN, **10**, No. 3 (2008).
2. Andreev I.A., Il'inskaya N.D., Kunitsina E.V., Mikhailova M.P., Yakovlev Yu.P., Fiz. Tekh. Poluprovod., **37**, No. 8 (2003).
3. Vincent J.D., Vampola J., Pierce G., Stegall M., Hodges S., Fundamentals of Infrared and Visible Detector Operation and Testing, Wiley, Hoboken (2015).
4. Jariwala D., Sangwan V.K., Lauhon L.J., Adv. Mater., No. 20, 939-946 (2008).
5. Merchant C.A., Markovic N., Appl. Phys., No. 243510, 92 (2008).
6. Zhang J., Xi N., Lai K., SPIE Newsroom, DOI: 10.1117/2.1200701.0514 (2007).
7. Pradhan B., Setyowati K., Liu H., Waldeck D.H., Chen J., Nanoletters, **8**, No. 4, 1142-1146 (2008).
8. Qingsheng Z., Sheng W., Leijing L., Opt. Mat. Express, **2**, No. 6, 839-848 (2012).
9. Jimmy X., ACS Nano, **2**, No. 10, 2154-2159 (2008).